Life on the edge: a beginner's guide to the Fermi surface



2016 Phys. Scr. 91 053009

(http://iopscience.iop.org/1402-4896/91/5/053009)

OPEN ACCESS
IOP Publishing | Royal Swedish Academy of Sciences Physica Scripta
Phys. Scr. **91** (2016) 053009 (13pp) doi:10.1088/0031-8949/91/5/053009

## Invited Comment

# Life on the edge: a beginner's guide to the Fermi surface

**S B Dugdale**

H.H. Wills Physics Laboratory, University of Bristol, Tyndall Avenue, Bristol BS8 1TL, UK

E-mail: s.b.dugdale@bristol.ac.uk

Received 30 November 2015, revised 22 March 2016
Accepted for publication 30 March 2016
Published 18 April 2016

**Abstract**

The concept of the Fermi surface is at the very heart of our understanding of the metallic state. Displaying intricate and often complicated shapes, the Fermi surfaces of real metals are both aesthetically beautiful and subtly powerful. A range of examples is presented of the startling array of physical phenomena whose origin can be traced to the shape of the Fermi surface, together with experimental observations of the particular Fermi surface features.

Keywords: electronic structure, Fermi surface, metals, positron annihilation, Compton scattering, nesting, quantum oscillations

(Some figures may appear in colour only in the online journal)

## 1. Introduction

For most of us, our first contact with a Fermi surface is through the Sommerfeld free electron model, a model in which it has a spherical shape. In real metals, however, the Fermi surface can be (and normally is) very different from a sphere (for example, the Fermi surface of Pb is shown in figure 1). Indeed, 'fantasies of a modern artist' is how Lifshitz and Kaganov describe the diverse forms that the Fermi surface has been shown to exhibit [1, 2], and the lexicon is full of exotic sounding names such as *superegg* and *tetracube* [3]. In the 50 years since Allan Mackintosh suggested that defining a metal as 'a solid with a Fermi surface' might be the most meaningful description that one can give [4], the concept of the Fermi surface has deservedly achieved great prominence in undergraduate physics courses, often with substantial focus on methods which can reveal its shape in real metals (e.g. the measurement of quantum oscillations [5]). While there is an appreciation that electrons at (or within an energy $\sim k_B T$ of) the Fermi surface are special because of the Pauli exclusion principle preventing electrons from deep in the Fermi sea from being easily excited (and thus making any contribution to the transport properties), many students (and even senior colleagues) are left wondering about the physical significance of particular Fermi surface shapes or features.

The importance of the Fermi surface can be extended to the influence its shape can have on the ability of electrons to screen perturbations. From the oscillatory exchange coupling at the heart of giant magnetoresistance through to shape memory phenomena and even superconductivity, the Fermi surface can influence a range of fascinating physical phenomena. As Kaganov and Lifshitz put it, the Fermi surface is 'the stage on which the 'drama of the life of the electron' is played out' [2]. The purpose of this article is to showcase some of the drama that can result from particular shapes of the Fermi surface.

### 1.1. A potted history of the Fermi surface

Soon after the emergence of quantum mechanics in the 1920s, the following decade saw its application to the problem of understanding the behaviour of electrons in solids [7]. The result, the so-called band theory of solids, stands proudly as one of the theory's great early achievements. Beginning with Sommerfeld's successful free electron model, a quantum



 

version of the earlier classical Drude theory, the next advance was Bloch's discovery, obtained by straightforward Fourier analysis, that letting the electrons feel a periodic potential resulted in wavefunctions which were still delocalised, but differed from free-electron plane waves by a modulating function which had the periodicity of the lattice. These Bloch electrons, whose wavefunctions were just modulated plane waves extending over the whole crystal, were described as being 'nearly free'. A further consequence of the Bloch theory was the opening up of energy gaps (due to Bragg reflection of the electron waves) at the Brillouin zone boundary. It was at this point that Wilson had the insight to explain the difference between metals and insulators [8, 9]. Although both contain electrons which are nearly free, in insulators the electrons are in fully filled bands, and a fully filled band cannot carry a current. Wilson was also to explain a semiconductor as an insulator in which the band gap was comparable to $k_BT$. A solid with partially filled bands, on the other hand, will be a conductor—and have a Fermi surface. Thus, while the Bloch theory explained why electrons feeling a periodic potential could remain delocalised (nearly free), Wilson could explain why not all solids are metals by showing that insulators are qualitatively different from metals, and not merely bad metals.

The Fermi surface is the surface in reciprocal space which separates occupied from unoccupied electron states at zero temperature. The dynamical properties of an electron on the Fermi surface largely depend on *where it is* on the Fermi surface, and the shape of the Fermi surface with respect to the Brillouin zone can be a guide to the electrical properties of a metal [10].

A comprehensive and highly influential review by Sommerfeld and Bethe on the electron theory of metals was published in the *Handbuch der Physik* [11]. This article, described by Mott as 'astonishingly complete' [12] contained a number of sketches of 'Flächen konstanter Energie in Raum der Wellenzahlen', *surfaces of constant energy in the space of wavevector components*. Bethe later recalled [13]: 'It was clear to me … that it made a great difference whether the Fermi surfaces were nearly a sphere or were some interesting surface.' At the University of Bristol, Mott had recently been appointed to the chair of theoretical physics, and considered it his job to apply quantum mechanics to the experimental work that was in progress there [12]. Mott, and his Bristol colleagues, Jones and Skinner, began to wonder about those energy surfaces, and whether they were merely a 'mathematical fiction' given that the nearly free electron theory ignored the Coulomb interaction between electrons [12]. In a real metal, would these energy surfaces be smeared out? Skinner's measurements of x-ray emission, performed with O'Bryan, answered that question by showing very sharp cut-offs in the emission intensity at high energy, indicating that the energy surface did remain sharp [14]. At the same time, the terminology in a paper by Jones and Zener [15] evolves from a purely mathematical concept ('the surface of the Fermi distribution function') at the beginning of the article to the more physically tangible 'Fermi surface' by the end. The term 'Fermi surface' stuck. It would, however, take another twenty years before Landau's theory of the Fermi Liquid and the experimental observation of the Fermi surface of Cu would put the existence of a sharp Fermi surface on firm ground. Today, the observation of a Fermi surface is perhaps the most important signature of the existence of Fermi liquid quasiparticles in a material.

### *1.2. Quantum oscillations and the Fermi surface of Bi*

Oscillations as a function of magnetic field in the magnetic susceptibility of Bi were observed by de Haas and van Alphen in 1930 [16]. Now known as the de Haas–van Alphen (dHvA) effect, the observation of such oscillations has evolved into one of the most powerful probes of the Fermi surface, but at the time there was no theory to understand this behaviour. Using Landau's ideas about energy levels in a magnetic field [17], Peierls was able to develop a quantitative theory based around these 'Landau levels' passing through the chemical potential [18]. In 1938, Schoenberg's detailed measurements of quantum oscillations in Bi performed during a stay in Moscow with Kapitza, interpreted with the aid of 'in-house' theoretical insight from Landau, delivered the first determination of a Fermi surface [19]. This did not, however, immediately lead to an explosion of results in other metals, the widely held belief being that in practice the effect would only be observable in Bi. It was not until 1947, and Marcus' observation of quantum oscillations in Zn [20], that Schoenberg and others started to look for the effect in other metals. The results, however, were incompatible with an ellipsoidal Fermi surface model, which was sufficiently good for Bi. It was Onsager who first published a simple interpretation of the periodicities of the dHvA oscillations which could be related to the size of the Fermi surface [21]; although he had not published, the same idea had been developed by Lifshitz independently, and the theory was presented in greater detail together with Kosevich [22]. Looking forward more than half a century, this theory has enabled the Fermi surface of unconventional superconductors such as $Sr_2RuO_4$ [23, 24] and $UPt_3$ to be determined [25, 26], mapping not only their complex shapes but also revealing the quasiparticle masses for comparison with thermodynamic measurements such as specific heat. Back in the 1950s, a new and exciting age of discovery—a golden age of fermiology—was about to begin.

### *1.3. The experimental determination of the Fermi surface of Cu*

The crystalline state is not isotropic, and the presence of a finite potential (from the electron–ion interaction, and the effective Coulomb repulsion between electrons) modifies the shape of the bands so that their energies no longer have to depend quadratically on the wavevector, and the Fermi surface can distort from the free-electron sphere. Indeed, as previously emphasised, the Fermi surfaces of real metals are not spherical.

For a sufficiently pure metal at low temperature, high frequency oscillations of an electric field and the resulting current are confined to a layer within the surface to a depth much less than the mean free path [27]. For a given (constant)

high frequency, the surface resistance tends to a constant value (the so-called extreme anomalous limit) which can be a complicated function of orientation for an anisotropic metal. Sondheimer and Pippard were able to show how the anisotropy of the high-frequency surface resistance of a metal could be related to the curvature of the Fermi surface [28–30]. Subsequently, Pippard went on to determine the Fermi surface of Cu (chosen for its 'metallurgical convenience') from measurements made on twelve carefully cut and polished single crystal samples [31]. Shortly afterwards, Garcia-Moliner showed that the Fermi surface was compatible with a tight-binding energy band for a face-centred cubic lattice which included next-nearest-neighbour interactions [32]. Early band structure calculations by Segall and Burdick [33, 34] were broadly consistent with Pippard's results, and with the subsequent measurement of dHvA oscillations by Schoenberg [35], which were quickly parameterised by Roaf [36].

Today there is a wide range of techniques for measuring the Fermi surface. Being able to map out the shapes of Fermi surfaces in disordered alloys and at higher temperatures [37–39], positron annihilation [40] (including spin-resolved positron annihilation [41]) and Compton scattering [42] have come a long way since the pioneering experiments of Berko and Plaskett [43]. The rise of angle resolved photoemission spectroscopy (ARPES) in recent years has also broadened the fermiologist's arsenal, beautifully revealing both Fermi surfaces and band dispersions [44], and including the possibility of spin-polarised measurements [45].

## 2. Why is the shape of the Fermi surface important?

### *2.1. The Fermi surface interaction with the Brillouin zone boundary*

Reminiscing about the early 1930s in Bristol, Mott observed: '*It was a revelation to me that quantum mechanics could penetrate into the business of the metals industry*' [46]. What is the significance of the Fermi surface approaching and making contact with the boundary of the Brillouin zone? A Brillouin zone can hold two electrons (one of each spin) per primitive unit cell, and thus within the free electron model it is straighforward to calculate the Fermi wavevector $k_{\rm F}$ for a given number of electrons (and thus how close it comes to the Brillouin zone boundary).

In 1933, Jones heard Bragg speak about the structure of metallic alloys and in particular about the work of the Oxford metallurgist, Hume-Rothery [47] who had made a connection between the structures of some brasses and bronzes and their valence electron per atom ratios (denoted as $e/a$) [48]. Jones began to think about explaining this in terms of the proximity of the Fermi sphere to the Brillouin zone boundary; at the zone boundary, there is the well-known energy gap associated with the Bragg reflection of the electrons, and the gradient of energy band flattens out as it approaches the faces of the Brillouin zone [49]. By making model calculations of the density of states for some fcc and bcc alloys, and evaluating the band energies, Mott and Jones went on to show that fcc would be favoured for electron per atom ratios $e/a \leqslant 1.44$ and bcc for larger ratios. Thus the proximity of the Fermi sphere to a Brillouin zone will lower the band energy of the metal. In 1937, Jones made some more sophisticated calculations using a nearly free electron model [50]. These calculations predicted the fcc/bcc transition would be at $e/a = 1.41$, but the $e/a$ ratios corresponding to peaks in the nearly free electron density of states were well away from the critical ratio, undermining the appealingly intuitive arguments of the original Mott–Jones theory [51].

It was after Pippard discovered the necks in the Fermi surface of Cu (revealing the real, non-spherical Fermi surface had already made contact with the zone boundary at an $e/a$ ratio of 1.0) that the problem with the Mott–Jones model became even more apparent. Fermi surfaces of real metals are not spherical, and the rigid band model (where the Fermi energy is rigidly moved up or down depending on the electron concentration) is crude and often widely inappropriate [52]. Indeed, given the strong deviation of the real Fermi surface of Cu from the free-electron sphere, it is astonishing how well the Mott–Jones theory, of Fermi spheres touching the Brillouin zone boundary, worked. There is no special significance to the $e/a$ ratio at which the *real* Fermi surface touches the Brillouin zone boundary, but the $e/a$ ratio at which the free-electron sphere touches the boundary provides a useful indication [51].

Current ideas about the microscopic origin of the Hume-Rothery rules can be traced to the speculations of Blandin, Heine, Ashcroft and Stroud that there will be a particular stability associated with the Fermi surface approaching the Brillouin zone boundary due to the band energy dropping rapidly as the Fermi surface caliper $2k_{\rm F}$, changing with $e/a$, passes through a reciprocal lattice vector [53–56]. These ideas were later put on a firm mathematical foundation by Evans *et al* [57]. To understand the connection with $2k_{\rm F}$, it is essential to appreciate how the shape of the Fermi surface can influence the screening properties of electrons.

### *2.2. Screening and the shape of the Fermi surface*

One of the most important ways in which the shape of the Fermi surface has a particular influence on physical properties of a metal is through its impact on electron screening. The response of the electrons to a perturbation of wavevector $\mathbf{q}$ and frequency $\omega$ can be encapsulated in a bare dynamical susceptibility, $\chi^0(\mathbf{q}, \omega)$:

$$\chi^0(\mathbf{q}, \omega) = \sum_{i,j,\mathbf{k}} \frac{f_{i\mathbf{k}}\,(1 - f_{j\mathbf{k}+\mathbf{q}})}{\epsilon_j(\mathbf{k}+\mathbf{q}) - \epsilon_i(\mathbf{k}) - \hbar\omega} \times |M_{i\mathbf{k},j\mathbf{k}+\mathbf{q}}(\mathbf{q})|^2, \quad (1)$$

where $i$, $j$ are band indices, $f$ is the Fermi–Dirac distribution function, $\epsilon(\mathbf{k})$ is the electron energy band dispersion and $M_{i\mathbf{k},j\mathbf{k}+\mathbf{q}}$ are matrix elements of the form

$$M_{i\mathbf{k},j\mathbf{k}+\mathbf{q}}(\mathbf{q}) = \langle \psi_{i\mathbf{k}} | e^{-i\mathbf{q}.\mathbf{r}} | \psi_{j\mathbf{k}+\mathbf{q}} \rangle. \quad (2)$$

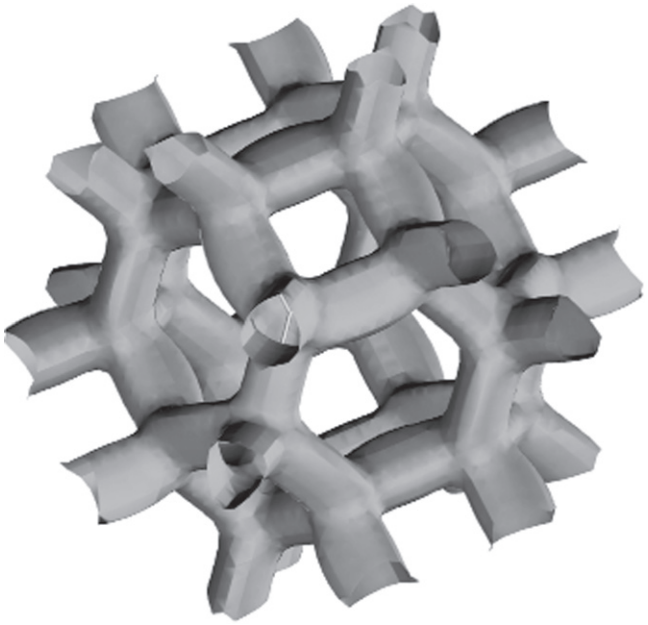

**Figure 1.** The Fermi surface of Pb, inspiration for Tony Smith's sculpture *For Dolores* (also called *Flores para los muertos*) [6].

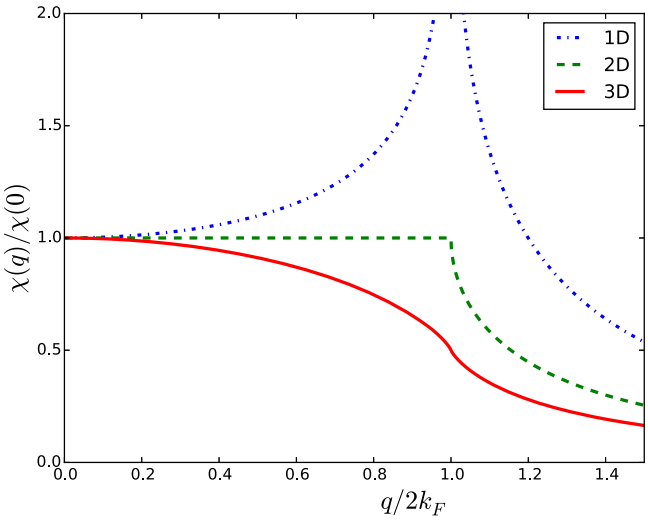


**Figure 2.** $\chi(\mathbf{q})/\chi(0)$ for a one-, two- and three-dimensional free electron gas.

In effect, $\chi^0(\mathbf{q}, \omega)$ determines how effective the electron screening response will be for a particular frequency $\omega$ and wavevector $\mathbf{q}$. The presence of a Fermi surface, a discontinuity in the occupation of the Brillouin zone, will introduce singularities into $\chi^0(\mathbf{q}, \omega)$, and these singularities will be reflected in the abilitiy of electrons to screen pertubations.

The bare static ($\omega = 0$) susceptibility ratio $\chi^0(\mathbf{q})/\chi^0(\mathbf{0})$ for a one-, two- and three-dimensional free electron gas are shown in figure 2. While the singularities in one- and two-dimensions are clear to see, in three-dimensions there is a logarithmic singularity in its derivative (i.e. the *slope* diverges) with respect to $q$ [58]. Of course, the energy bands of real metals deviate from the free electron parabolæ, and the Fermi surfaces are not spheres.

In many cases, the matrix elements are not included in the evaluation of $\chi^0(\mathbf{q}, \omega)$ (or set to be constant) and this is known as the constant matrix element approximation. The consequences of such an approach can be surprisingly severe (an example can be found below in the context of the spin-density wave; SDW antiferromagnetism of Cr) [59].

### 2.3. Electrons and phonons

One can imagine that a phonon with a wavevector $\mathbf{q}$ establishes a potential which the electrons will then try to screen so that the ions are effectively interacting with each other through this screened potential, modifying the forces between them and hence the frequency. Kohn pointed out that singularities in the electronic response $\chi(\mathbf{q}, \omega)$ may show up in phonon spectra [60], and suggested that the shape of the Fermi surface could be inferred from the locations of singularities in the vibrational spectra. Soon afterwards, Brockhouse *et al* measured such 'images of the Fermi surface' in their phonon spectra for Pb [61, 62], interpreting their spectra in terms of a Fermi surface topology which appeared rather like that of free electrons [63]. However, although electron–phonon coupling is rather strong in Pb, in general these so-called 'anomalies' turn out to be quite weak for most metals.

It is not just the phonons, of course, that the electrons will attempt to screen. The indirect exchange interaction between localised magnetic moments via conduction electrons is described by the Ruderman–Kittel–Kasuya–Yosida (RKKY) mechanism [64–66]. Within a free electron picture, the $2k_F$ singularity in the bare susceptibility gives rise to oscillatory exchange coupling as a function of distance $R$ from the magnetic moment being screened (characterised by a periodicity of $2\pi/2k_F = \pi/k_F$) and decaying as $1/R^3$.

What happens away from the free electron model with its spherical Fermi surfaces? Taylor [67] examined the effect of the curvature of the Fermi surface on Kohn anomalies, and Afanas'ev and Kagan [68] examined the case of flat, that is to say nested Fermi surfaces. More generally, Fermi surface nesting describes the situation in which different sheets of Fermi surface, or different parts of the same sheet can be made to coincide through a translation of some particular $\mathbf{q}$-vector. The work of Roth *et al*, focused on the generalisation of the RKKY interaction to anisotropic Fermi surfaces [69], showing that for a nested Fermi surface, the interaction falls off more slowly with distance [69] as $1/R$ (rather than $1/R^3$). Fehlner and Loly showed that the logarithmic divergence in the bare susceptibility (coming from perfectly nested planar Fermi surfaces) evolves into a smooth peak for finite curvature.

The idea of mapping out the Fermi surface from these anomalies was explored by Weymouth and Stedman who investigated some particular calipers (extremal vectors) in the Fermi surface of Al [70]. They concluded that as a procedure for determining the Fermi surface, results would be difficult to interpret without access to any additional information, and

that (of course) strong electron–phonon coupling and large flat nested areas would make the anomalies easier to observe.

### 2.4. SDW antiferromagnetism and spin excitations

Overhauser predicted that the electron gas would be unstable with respect to the formation of a SDW with a wavevector $Q = 2k_F$ and suggested that the antiferromagnetic ground state of Cr is in fact such a SDW [71, 72]. Indeed, the electronic structure calculations of Lomer showed that Cr had a Fermi surface in which two of the sheets, an electron octahedron at the Γ-point and a hole octahedron at the $H$ point, were *almost perfectly* nested [73]. The fact that the sizes of the two octahedra are slightly different gives rise to the small incommensurability of the SDW which can be described by $\mathbf{Q} = \frac{2\pi}{a}(1 \pm \delta, 0, 0)$ [74]. The inclusion of matrix elements in the bare susceptibility calculations was shown to be rather important, as both Cr and Mo have very similar Fermi surface topologies (suggesting that they might both support SDWs), but the inclusion of matrix elements strongly suppresses the peak at the nesting vector in Mo [75]. Doping Cr with small concentrations of Mn (which adds electrons, growing the electron octahedron to reduce the mismatch in size) reduces $\delta$, while doping with small concentrations of V increases $\delta$ (since V has fewer electrons and thus worsens the mismatch in octahedron size) [76]. This behaviour was reproduced in the bare susceptibility calculations of Schwartzman *et al* [75].

Even when there is no long range magnetic order, the Fermi surface can play a role in promoting spin fluctuations. A good example of a material where this is thought to be important is $Sr_2RuO_4$, which has been proposed as a chiral $p$-wave superconductor (see [77] for a review). The bare susceptibility, calculated by Mazin and Singh, shows four peaks connected by weaker ridges [78] due to the nested Fermi surface topology, and incommensurate peaks and ridges of magnetic fluctuations have been observed by inelastic neutron scattering [79].

### 2.5. Friedel oscillations

Just as the RKKY indirect exchange interaction describes the oscillatory behaviour of the screening electron spins, Friedel oscillations refer to the characteristic oscillations in the screening charge around a charge impurity [80].

With the development of scanning-tunnelling miscroscopes (STMs), it has been possible to observe Friedel oscillations on metallic surfaces. It is worth noting that the lower dimensionality of the surface enhances the susceptibility singularity, making the oscillations easier to observe. The 'surface' Fermi surface of a Cu (111) surface (as distinct from the bulk Fermi surface) is a circle with a radius of $k_F = 0.215$ Å$^{-1}$ [81]. Thus one would expect to see oscillations with a spatial period of $\pi/k_F$ or ≈15Å, and such oscillations were observed around point defects on a Cu (111) surface by Crommie *et al* in their STM images [82].

Weismann *et al* exploited the anisotropy of the Friedel oscillation created by Co impurities on Cu surfaces (due to the variation of curvature over the Fermi surface) to make inferences about the shape of the Fermi surface, in effect 'seeing the Fermi surface in real space' [83, 84].

### 2.6. Charge-density waves (CDWs)

The Peierls transition is an electronic instability at zero temperature in a one-dimensional crystal which occurs because of the perfect nesting in a one-dimensinal Fermi 'surface'. For a long time, CDWs in metals were commonly interpreted within the Peierls picture, associating the appearance of CDWs in metals with the presence of nesting in the Fermi surface. A very important contribution of Mazin and Johannes [85] cast doubt on whether, in anything other than one-dimension (which was where Peierls first made his observation), Fermi surface nesting could be responsible for the formation of CDWs. They pointed out that even in one-dimension, the Peierls mechanism is very weak. Recently Zhu *et al* [86] have suggested a reclassification of CDWs based on the mechanism behind their formation. Within this scheme, type I CDWs would fit the Peierls picture with Fermi surface nesting behind the transition, whereas type II would be associated with **q**-dependent electron–phonon coupling.

### 2.7. The shape of the Fermi surface and superconductivity

In the Bardeen–Cooper–Schrieffer theory of superconductivity, the attractive pairing interaction between electrons is mediated by phonons [87]. However, it was soon pointed out (e.g. [88]) that pairing could occur in higher angular momentum channels than $l = 0$ (not $s$). For these channels, the long-range attractive part of the interaction can dominate the short-range repulsion, providing a route to superconductivity. In 1965, Kohn and Luttinger [89] pointed out that a sharp Fermi surface will result in an oscillatory interaction potential (just as in the case of the RKKY interaction or Friedel oscillations discussed earlier), suggesting that the electrons could make use of the attractive parts of the interaction to form Cooper pairs and exhibit superconductivity. The key ingredient is that if the superconductivity has an *unconventional* gap function which changes sign, then the repulsive Coulomb interaction can be minimised.

Moving away from interactions between charges, Berk and Schrieffer began to consider pairing interactions between electron *spins* [90], and the possibility of superconductivity mediated by spin-fluctuations. Imagine that the first electron, let us say a spin-up electron, antiferromagnetically polarises the electrons around it creating a local region of spin-down electrons. Then a spin-down electron can lower its energy by being in that region of electrons with the same spin. By having a pairing wavefunction which has a node at the origin (e.g. $d_{x^2-y^2}$, pertinent to the cuprates [91]), the Coulomb repulsion is minimised; whereas the retarded electron–phonon interaction keeps electrons apart in time, here they are kept apart in space. The Fermi surface shape (and any nesting) is important for superconductivity, and enters through a pairing interaction that depends on $\chi(\mathbf{q})$ [92–94].

In the case of the Fe-pnictide superconductors, where there is more than one sheet of Fermi surface [95], the possibility of nesting between electron and hole sheets means that a pairing state which retains *s*-wave symmetry can exist provided that the gap function has different signs on the two sheets; this is known as an extended *s*-wave or $s^{+-}$ state [96–98].

### 2.8. Compositional and magnetic short-range order

A powerful example of the impact of Fermi surface nesting is in the compositional short-range order found in some disordered alloys. Compositional order within an alloy refers to periodicities in the occupation of sites by particular species of atoms. Such correlations may be long range (for example, an ordered $Cu_3Au$ structure) or short range. Moss pointed out that there should be a phenomenon, equivalent to the Kohn effect in the phonon dispersion, which gives rise to compositional short-range order in concentrated disordered alloys [99]. In what is known as the Krivoglaz–Clapp–Moss theory [100–103], the singularity in the bare susceptibility will also appear in the Fourier transform of the pairwise interatomic potential, driving concentration waves. The short-range order gives rise to diffuse scattering (i.e. scattering not associated with a Bragg peak) in the electron diffraction patterns in disordered $Cu_{1-x}Pd_x$ alloys [104, 105]. At this point it is appropriate to pause and consider whether the Fermi surface remains a meaningful concept in a substitutionally disordered alloy. In a periodic potential, the Bloch wavevector $\mathbf{k}$ is a good quantum number and the lifetime of a Bloch electron is infinite. Disorder means additional scattering (which will change the wavevector) and thus the wavevector $\mathbf{k}$ is no longer a good quantum number and the lifetime becomes finite. There is, however, substantial theoretical (see, for example, [106, 107]) and experimental evidence that the concepts of Brillouin zones and Fermi surfaces remain robust in such alloys. Although the Fermi surfaces in substitutionally disorded alloys can be rather smeared (due to the disorder), the Krivoglaz–Clapp–Moss theory was able to explain the observed diffuse scattering in terms of a nested Fermi surface [99, 100]. Later, Györffy and Stocks were able to quantitatively connect the observed short-range order with the nesting of the Fermi surface [108], and Wilkinson *et al* were able to observe the nested regions (figure 3) using positron annihilation [109]. The Fermi surface, through its nesting influencing the electronic screening, is determining the compositional ordering of the atoms.

In $PdCrO_2$, a rare example of a two-dimensional triangular lattice antiferromagnetic metal, the magnetic interactions are frustrated [110]. The presence of nesting in its paramagnetic Fermi surface is likely to be at least partly responsible for the diffuse *magnetic* scattering observed above the Néel temperature [111] i.e. the Fermi surface can also promote magnetic short-range order with the electrons screening the magnetic interactions.

### 2.9. The RKKY interaction and oscillatory exchange coupling

All the heavy rare-earths with partially filled 4f bands have magnetic moments which order in periodic arrangements which are in general incommensurate with the lattice [112], and it was Williams *et al* [113] who first made explicit the connection between the magnetic order and a particular part of the Fermi surface (known as the 'webbing'), building on earlier ideas [114, 115]. The exception is Gd, which does not have the 'webbing' and orders ferromagnetically, but the other heavy rare-earth elements display a fascinating range of antiferromagnetic ordering [116].

The idea is that the 4f electrons form very localised magnetic moments (which are too far apart for there to be any signficant direct exchange between the 4f wavefunctions). However, these moments are then screened by the conduction (s–d) electrons, giving rise to an exchange coupling which oscillates as a function of distance from the magnetic moment. Neighbouring magnetic moments then experience (and are influenced by) an effective magnetic field carried by the s–d conduction electrons (figure 4).

The electronic structure of the two elements Y and Sc are often closely linked with the heavy rare earths, as they possess the same *hcp* structure as them and very similar Fermi surfaces. The first calculation of the Fermi surface of Y was by Loucks [117]. An experimentally determined Fermi surface of Y, obtained by positron annihilation measurements [118] is shown in figure 5, with the nested region coined the 'webbing' indicated by a double-headed arrow.

For dilute concentrations of Tb in Y–Tb alloys (between 2 and 7 at% Tb), the 4f Tb moments order in helical antiferromagnetic arrangement. The interlayer turn angle of the helix (which describes the rotation of the moment between successive moments along $c$) tends towards a value of 50° [119] (see figure 5). The interlay turn angle in degrees, $\theta$, is related to the magnitude of the wavevector $q$ (expressed as a fraction of $2\pi/c$) of the modulation by $\theta = q \times 180$. Thus a $q$ vector of $0.28 \times 2\pi/c$ will give an interlayer turn angle of about 50°. Caudron *et al* were able to measure the ordering of Er moments within a dilute (0.5–3 at% Er) Y–Er alloy [120]. Long range incommensurate antiferromagnetic order was observed, with a modulation vector of $0.27 \times 2\pi/c$.

Moving towards a microscopic theory of the magnetic ordering in the heavy rare earths, by making calculations of the bare static susceptibility using realistic band structures, Evenson and Liu were able to show that the 'webbing' Fermi surfaces generated peaks in $\chi^0(\mathbf{q})$ at wavevectors which were close to the observed magnetic ordering vectors [121, 122].

The 'webbing' was clearly observed in the positron annihilation measurements of Dugdale *et al* [118], a study which was subsequently extended to the Gd–Y alloy system. By measuring the Fermi surface of a series of disordered alloys, a connection could be made between the presence of such a 'webbing' and antiferromagnetic order [123]. The induced spin polarisation on the Y electrons (which are communicating the RKKY-like coupling between Gd moments) was later observed through magnetic Compton scattering [124]. The 'webbing' has also been observed by

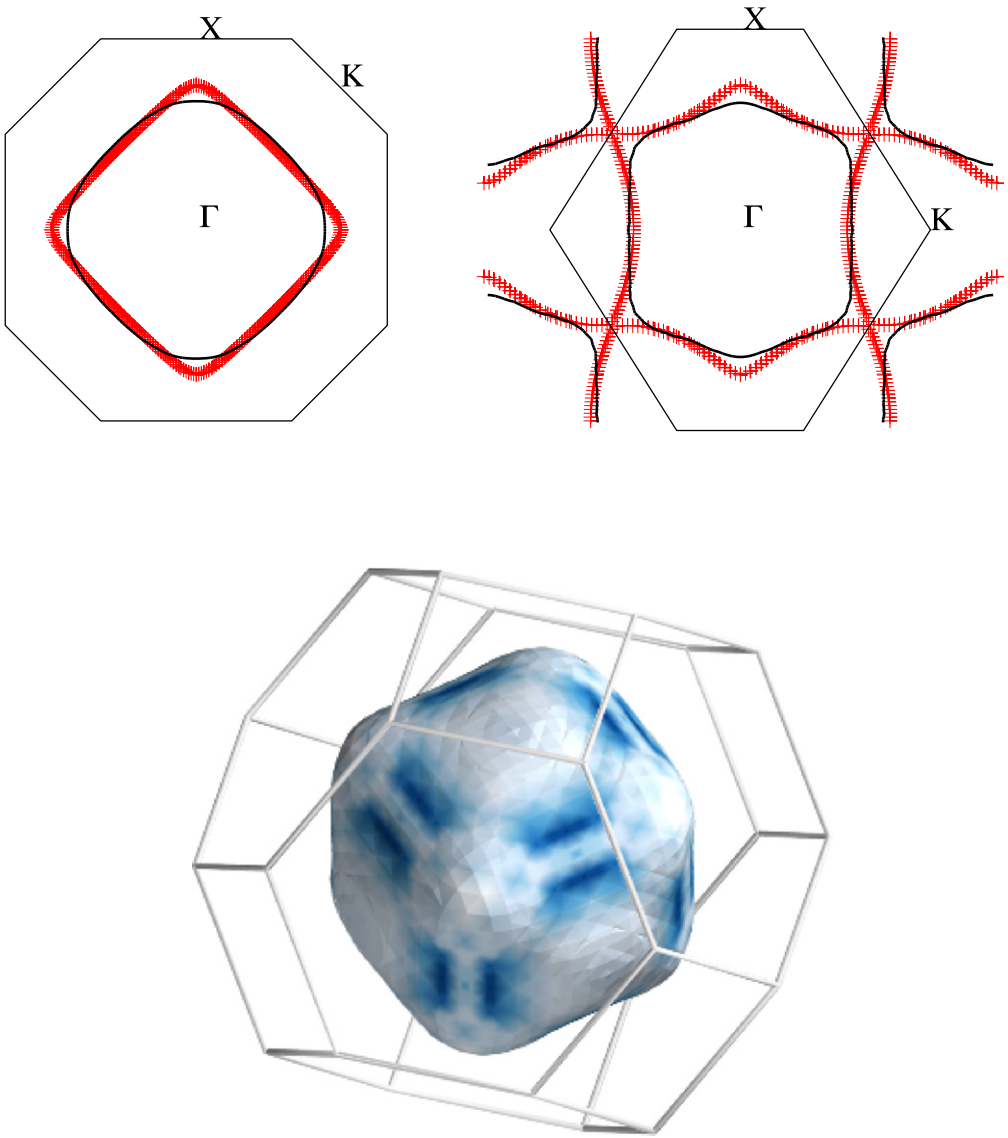


**Figure 3.** Top: two planes through the Fermi surface of $Cu_{0.6}Pd_{0.4}$. The experimental data are shown as solid lines within the first Brillouin zone, and the crosses are from KKR-CPA calculations. Bottom: Fermi surface reconstructed from positron annihilation data, on which the shading indicates the nested regions. For details of the experiments and calculations, see [109].

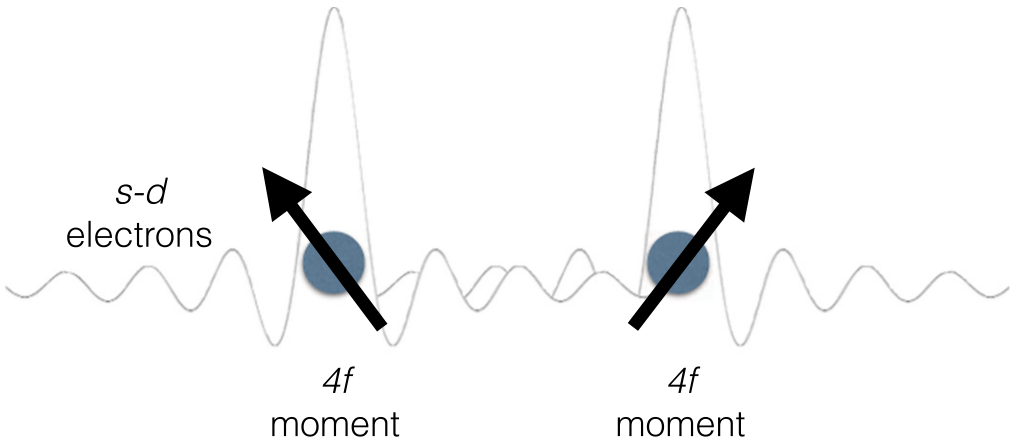


**Figure 4.** Schematic of the RKKY indirect exchange interaction between localised 4f moments. Around each 4f moment the itinerant s–d electrons will attempt to screen the localised magnetic moment, resuling in an oscillatory spin density.

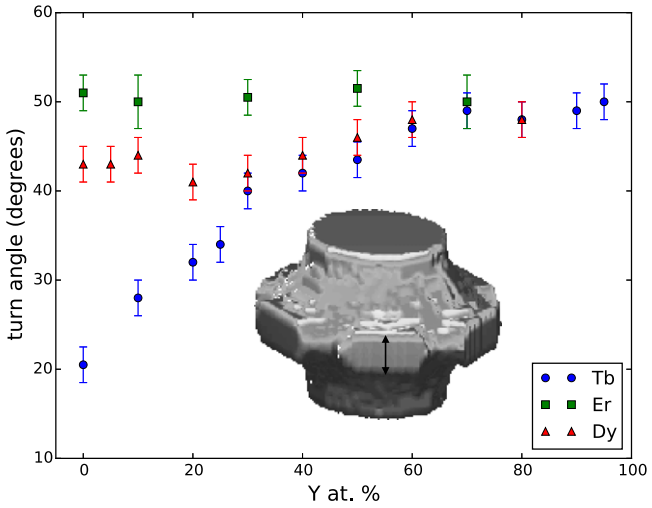


**Figure 5.** The interlayer turn angle for a series of alloys of Y with Tb, Dy and Er. The data were extracted from [119]. The Fermi surface of Y measured by positron annihilation is also shown, with the double-headed arrow spanning the region known as the 'webbing' [118].

ARPES in Tb and Dy [125, 126], and its absence observed in Gd [127].

More recently, Hughes *et al* have been able to explain the magnetic ordering in the heavy rare earths, within a first-principles framework, through the influence of the $c/a$ ratio of the hcp lattice and the cell volume on the bare susceptibility as a result of the propensity towards Fermi surface nesting [128].

Antiferromagnetic exchange coupling was observed by Majkrzak *et al* in Gd–Y [129] and by Grünberg in Fe/Cr [130], with an RKKY-like interaction mooted as a possible mechanism. These discoveries led swiftly to that of giant magnetoresistance [131] in 1988 [132]. In 1990, Parkin *et al* made the surprising discovery of long range oscillatory exchange coupling which depended on the thickness of the non-magnetic spacer layer [133]. The strong resemblance to RKKY oscillations guided Bruno and Chappert to propose [134] and develop a model [135] to explain the observations. Their model was based on an RKKY interaction between the ferromagnetic layers through the spacer layers, with the key point that the spacer layer thicknesses were discrete. By mapping the Fermi surface topologies of a range of Cr, Cr–V and Cr–Mo alloys, Hughes *et al* were able to track the evolution of one particular piece of Fermi surface (the hole ellipsoids located at the *N* points) and show its relationship to the periodicity of the oscillatory exchange coupling [136], as previously predicted by Lathiotakis *et al* [137].

### *2.10. Electronic topological transitions*

Lifshitz was the first to point out that there would be anomalous behaviour in thermodynamic, elastic and transport properties if, by varying some thermodynamic variable, the chemical potential passes through a stationary point in the band structure (a van Hove singularity [138]). At such a point, the connectivity of the Fermi surfaces changes [139]. The transition could, for example, be achieved by changing the electron per atom ratio by alloying, or by applying pressure or uniaxial stress. The four basic types of change in connectivity are the opening up or closing of electron or hole pockets, or the formation or pinching off of a neck [140]. Within the Ehrenfest scheme, Lifshitz classified such a transition at $T = 0$ as a $2\frac{1}{2}$ order phase transition, but it should be noted that it is not a phase transition at finite temperature; both temperature and disorder would turn any divergences in quantities such as the thermopower into finite peaks [140].

For a general review, see [140] and for some examples of Fermi surfaces undergoing ETTs, see [141]. Another couple of illustrative examples are related to metamagnetic transitions [142] which can be empirically defined as a supralinear rise in the magnetisation at some particular value of applied magnetic field. In some heavy fermion systems, the Fermi surface appears to evolve under an applied magnetic field (see, e.g. [143, 144]) which is to say that there are Zeeman-driven ETTs. URhGe is worthy of attention because superconductivity and ferromagnetism appear to coexist [145], suggesting triplet equal-spin Cooper pairs. Application of a magnetic field initially kills the superconductivity, but it reappears at high field [146]. Its Fermi surface was measured by Yelland *et al* [147], and by tracking how it evolved as a function of applied magnetic field they concluded that the field was inducing an ETT, and were able to follow the disappearance of a minority spin Fermi surface pocket with a Fermi velocity ($v_F$) which also falls to zero at the ETT. Hall coefficient changes at the re-entrant magnetic field agree with this picture of the disappearance of a heavy (small $v_F$) sheet at the re-entrant field [148].

$Sr_3Ru_2O_7$ also exhibits metamagnetic behaviour [149], and there appears to be an intimate connection between field-induced changes in the Fermi surface across the metamagnetic transition (most likely due to a van Hove singularity close to the Fermi energy) and the presence of a SDW [150]. It is likely that the presence of a SDW could be associated with appearance of a nested Fermi surface.

In the Fe-pnictide superconductors, the Fermi surface plays a significant role in the relationship between magnetism and superconductivty [95]. In $CaFe_2As_2$, for example, the tetragonal structure gives way to apparently concomitant SDW and orthorhombic transitions [151, 152] at 170 K. Under a small pressure, the transition is suppressed and superconductivity appears at low temperature [153], while under higher pressures a so-called 'collapsed tetragonal' ($cT$) phase emerges which is non-magnetic [154]. Recent studies (e.g. [155, 156]) have been able to connect the disappearance of the Γ-centred hole pockets at the $cT$ transition with the disappearance of magnetism and bulk superconductivity.

### *2.11. Phonon softening and shape memory alloys*

Shape-memory alloys exhibit the highly technologically useful property of being able to 'remember' their previous form when subjected to some external stimulus (e.g. stress, temperature) [157]. The behaviour is associated with a martensitic transformation below a certain temperature. These

transitions are, however, commonly preceded by 'precursor' or 'premartensitic' phenomena (e.g. strong phonon softening, diffuse scattering in electron diffraction) well above the actual martensitic transformation, and are believed to have a common origin associated with Fermi surface nesting [158]. Indeed, for the shape-memory alloy $\beta$-phase Ni–Al, calculations of the electronic structure and the phonon dispersions indicated that the softening was linked with a nesting feature in the Fermi surface [159], subsequently identified experimentally by Dugdale *et al* [160]. Similar conclusions were drawn for Ni–Ti [161] and in AuZn, Goddard *et al* [162] were able to infer a 'catastrophic' Fermi surface reconstruction at the martensitic transformation, consistent with theoretical predictions [163]. It should be emphasised that the martensitic transformation does not require there to be Fermi surface nesting (the structural transition would happen anyway), but nesting can play a supporting role.

There also exist *ferromagnetic* shape memory alloys, of which the Heusler alloy $Ni_2MnGa$ is the most well-known example [164]. For these alloys, an external magnetic field can provide the stimulus required for the alloy to change its shape. With a Curie temperature of about $T_c \sim 380$ K, the premartensitic and martensitic transformations occur within the ferromagnetic state ($\sim$250 K and $\sim$220 K, respectively). The exchange splitting, and therefore the Fermi surface topology will be evolving as a function of temperature, something not taken into account in earlier investigations of Fermi surface nesting [165]. This inspired Lee *et al* to calculate the bare susceptibility as a function of the saturation magnetisation [166] and implicate one particular nested sheet of Fermi surface in promoting the premartensitic phonon softening [167], and preparing the system for the eventual martensitic transformation. Experimentally, the Fermi surface of $Ni_2MnGa$ was revealed by the positron annihilation experiments of Haynes *et al* [168], revealing nesting vectors that could be compatible with the premartensitic ordering as well as the so-called '5M' martensite.

### *2.12. Fermi surfaces of the quarternary rare earth borocarbides*

The interplay of magnetic order and superconductivity in the quarternary borocarbides have led them to be described as a 'toy box for solid-state physicists' [169]. They have the general formula $RNi_2B_2C$, where $R$ is a rare earth element (or Lu/Y). Discovered in the mid 1990s [170, 171], they have relatively high superconducting transition temperatures (e.g. $LuNi_2B_2C$ has a $T_c$ of 16.6 K [170]). The anisotropy of the superconducting gap, and some indication of other unconventional features such as point nodes, has meant that multiband superconductivity has not been ruled out [172].

The paramagnetic Fermi surfaces for different $R$ can be expected to be very similar since the the filling of the $f$ bands does not strongly influence the bands near the Fermi energy. When the rare earth $R$ is Er, Tb or Gd, incommensurate antiferromagnetic order was found with a characteristic wavevector parallel to the $a*$ direction of magnitude $\sim 0.55 \times \frac{2\pi}{a}$ [173–177]. Furthermore, it was noticed that the phonon spectrum showed strong temperature-dependent softening along [100], at about the same $\mathbf{q}$ [178]. Calculations of the bare susceptibility revealed a peak at the same wavevector, the origin of which was a prominent nesting feature in one Fermi surface sheet [179]. The observation of an increase in the nuclear magnetic resonance relaxation rate at low temperatures has been interpreted as being indicative of the presence of strong antiferromagnetic spin fluctuations [180], which are likely be be enhanced by Fermi surface nesting. It is believed that importance of the crystal electric field for the magnetic interactions when the rare earth is Dy or Ho explains the absence of an $a*$ propagation vector [181].

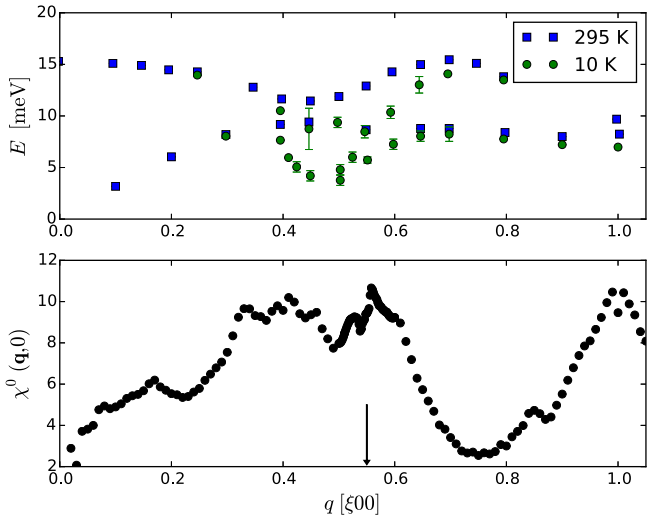


**Figure 6.** Top: softening of the $\Delta_4$ [$\xi$00] phonons in $LuNi_2B_2C$ between 295K and 10K. The data have been taken from [178]. Bottom: calculation of the $\chi^0(\mathbf{q}, 0)$ for the nested Fermi surface sheet, with the arrow indicating the wave vector associated with the magnetic order in $ErNi_2B_2C$ [173, 174], $TbNi_2B_2C$ [175, 176], and $GdNi_2B_2C$ [177].

Figure 6 shows how the shape of the Fermi surface, through its nesting properties, can be related to both phonon softening and magnetic order. The phonon softening identified from inelastic neutron scattering [178] has been reproduced (from the orginal data presented), together with a calculation of $\chi^0(\mathbf{q}, 0)$ for the nested Fermi surface sheet (which agrees with that of Rhee *et al* [179]). It is clear that the softening is very profound around the nesting vector, but it is still possible that this pronounced softening (over a range of wavevectors) is due to the $\mathbf{q}$-dependence of the electron–phonon coupling rather than Fermi surface nesting [182]. Note that the peak in the susceptibility coincides with the magnetic ordering vector when the rare Earth is Er, Tb or Gd.

This Fermi surface has been measured, and the nesting verified using positron annihilation [183, 184], and later by ARPES [185]. The nesting feature (identified most clearly from the full three-dimensional reconstruction of the Fermi surface by Utfeld *et al* [184]) can be seen in figure 7, and was determined to be $0.54 \pm 0.02 \times \frac{2\pi}{a}$ [183]. The nested area is rather small (extending as it does over some small range of $k_z$, see figure 3 of [184]), but the density of states there is rather large thus increasing its significance.

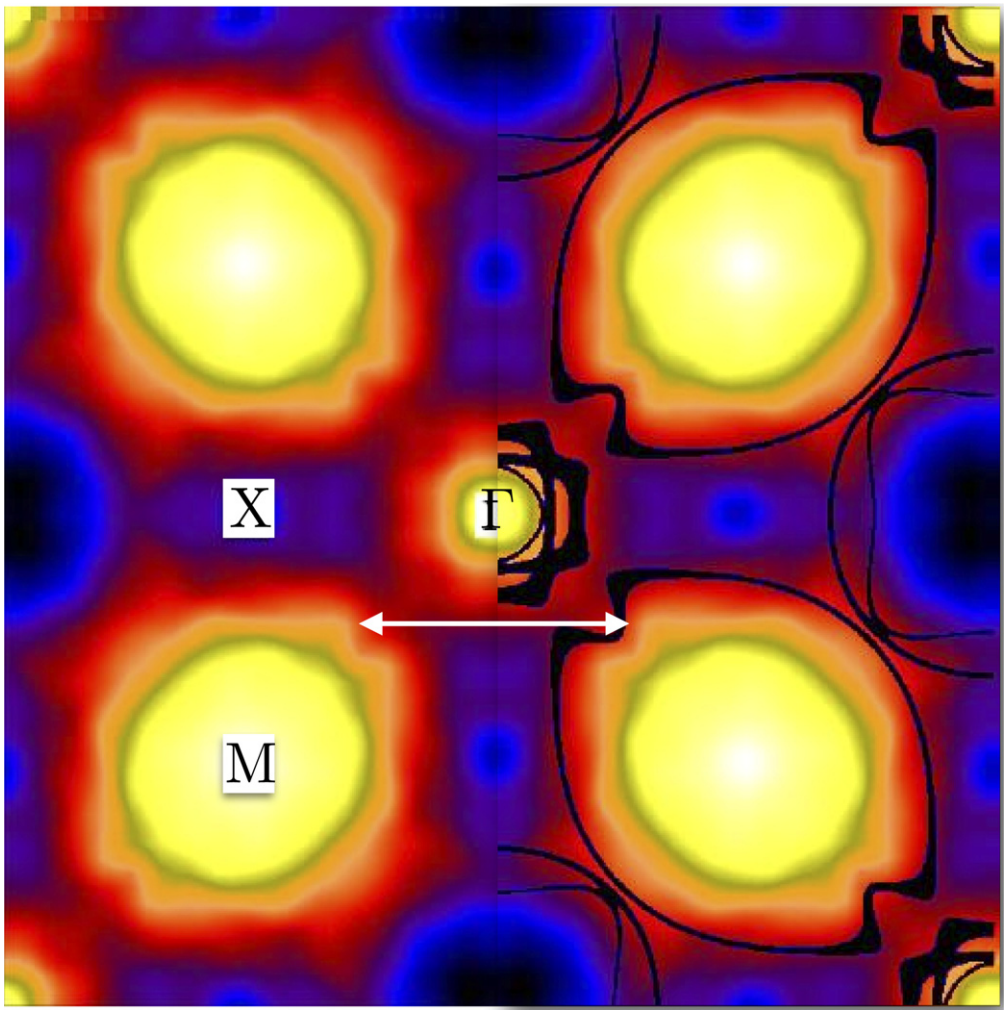


**Figure 7.** The electron occupation in $LuNi_2B_2C$ in an (001) plane through the Γ point of the Brillouin zone, measured by positron annihilation. Black is low occupation, white is high and the Fermi surface (indicated by the calculated Fermi surface overlaid as black lines on the right-hand side) is characterised by a change in occupancy. The nesting feature is indicated by the double-headed arrow.

## 3. Summary and perspectives

By presenting some of the physical phenomena associated with the existence of a Fermi surface, and emphasising the particular importance attached to its shape, the continuing importance of the fermiologist's endeavour has hopefully been made clear. In short, the Fermi surface has been shown to be the unifying concept behind a variety of electronic behaviours in metals. The examples of phenomena are not meant to be exhaustive, and indeed many interesting ideas have been omitted or only covered superficially (e.g. unconventional superconductivity). The Fermi surface is often the battleground for competing ordering phenomena, for example when superconductivity and CDWs appear to fight for control of the Fermi surface in $YBa_2Cu_3O_{6.67}$ [186].

Much of the discussion has focused on understanding things that happen as a result of features of the Fermi surface topology. It is also possible to think about tuning the electronic structure (for example via doping, or through the application of pressure or magnetic field) to engender specific properties. A great example to conclude with is the idea of 'engineering' a nested Fermi surface by doping the delafossite $CuAlO_2$ in order to create a transparent superconductor, an idea suggested by Katayama-Yoshida *et al* [187].

## Acknowledgments

I am grateful to Professors Ashraf Alam and Michael Springford for introducing me to the Fermi surface as an undergraduate student, to Professor Thomas Jarlborg for teaching me about electronic structure calculations, and to my doctoral students over many years for sharing my passion for measuring Fermi surfaces using positron annihilation and Compton scattering.

## References

[1] Lifshitz I M and Kaganov M I 1980 Geometric concepts in the electron theory of metals *Electrons at the Fermi Surface* ed M Springford (Cambridge: Cambridge University Press)

[2] Kaganov M and Lifshits I 1979 *Sov. Phys.—Usp.* **22** 904
[3] Andersen O K and Loucks T L 1968 *Phys. Rev.* **167** 551–6
[4] Mackintosh A R 1963 *Sci. Am.* **209** 110–20
[5] Shoenberg D 1984 *Magnetic Oscillations in Metals* (Cambridge: Cambridge University Press)
[6] Smith T 1973–75 *For Dolores, also Called Flores Para Los Muertos (Flowers for the Dead)* (Dallas, Texas: Raymond and Patsy Nasher Collection, Nasher Sculpture Center)
[7] Hoddesdon L, Baym G and Eckert M 1992 The development of the quantum mechanical electron theory of metals *Out of the Crystal Maze: Chapters from the History of Solid-State Physics* ed L Hoddesdon *et al* (Oxford: Oxford University Press) 926–1933
[8] Wilson A H 1931 *Proc. R. Soc.* A **133** 458–91
[9] Wilson A H 1980 *Proc. R. Soc.* A **371** 39–48
[10] Ziman J M 1962 *Contemp. Phys.* **3** 321–33
[11] Sommerfeld A and Bethe H 1933 *Elektronentheorie der metalle Aufbau Der Zusammenhngenden Materie* (*Handbuch der Physik* vol 24/2) (Berlin: Springer) pp 333–622 ISBN 978-3-642-89260-8
[12] Mott N F 1984 *Rep. Prog. Phys.* **47** 909
[13] Bethe H A Interviewed by Lillian Hoddesdon on 29 April 1981 Niels Bohr Library & Archives, American Institute of Physics, College Park, MD USA http://aip.org/history-programs/niels-bohr-library/oral-histories/4505
[14] O'Bryan H M and Skinner H W B 1934 *Phys. Rev.* **45** 370–8
[15] Jones H and Zener C 1934 *Proc. R. Soc.* A **145** 268–77
[16] de Haas W J and van Alphen P M 1930 *Proc. Neth. R. Acad. Sci.* **33** 1106
[17] Landau L 1930 *Z Phys.* **64** 629–37
[18] Peierls R 1933 *Z Phys.* **80** 763–91
[19] Shoenberg D 1939 *Proc. R. Soc.* A **170** 341–64 ISSN 0080-4630
[20] Marcus J A 1947 *Phys. Rev.* **71** 559–559
[21] Onsager L 1952 *London Edinburgh Dublin Phil. Mag. J. Sci.* **43** 1006–8
[22] Lifshitz I M and Kosevich A M 1956 *Sov. Phys.—JETP* **2** 636
[23] Bergemann C, Julian S R, Mackenzie A P, NishiZaki S and Maeno Y 2000 *Phys. Rev. Lett.* **84** 2662–5
[24] Bergemann C, Mackenzie A P, Julian S R, Forsythe D and Ohmichi E 2003 *Adv. Phys.* **52** 639–725
[25] Taillefer L and Lonzarich G G 1988 *Phys. Rev. Lett.* **60** 1570–3
[26] McMullan G, Rourke P, Norman M, Huxley A, Doiron-Leyraud N, Flouquet J, Lonzarich G, McCollam A and Julian S 2008 *New J. Phys.* **10** 053029
[27] Chambers R G 1952 *Proc. R. Soc.* A **215** 481–97
[28] Sondheimer E H 1954 *Proc. R. Soc.* A **224** 260–72
[29] Pippard A B 1954 *Proc. R. Soc.* A **224** 273–82
[30] Hoch P 1983 *Contemp. Phys.* **24** 3–23
[31] Pippard A B 1957 *Phil. Trans. R. Soc.* A **250** 325–57
[32] Garcia-Moliner F 1958 *Phil. Mag.* **3** 207–207
[33] Segall B 1962 *Phys. Rev.* **125** 109–22
[34] Burdick G A 1963 *Phys. Rev.* **129** 138–50
[35] Shoenberg D 1962 *Phil. Trans. R. Soc.* A **255** 85–133
[36] Roaf D J 1962 *Phil. Trans. R. Soc.* A **255** 135–52
[37] Major Z *et al* 2004 *Phys. Rev. Lett.* **92** 107003
[38] Laverock J *et al* 2007 *Phys. Rev.* B **76** 052509
[39] Utfeld C *et al* 2010 *Phys. Rev.* B **81** 064509
[40] Dugdale S B 2014 *Low Temp. Phys.* **40** 328–38
[41] Weber J A, Bauer A, Böni P, Ceeh H, Dugdale S B, Ernsting D, Kreuzpaintner W, Leitner M, Pfleiderer C and Hugenschmidt C 2015 *Phys. Rev. Lett.* **115** 206404
[42] Cooper M 1985 *Rep. Prog. Phys.* **48** 415
[43] Berko S and Plaskett J S 1958 *Phys. Rev.* **112** 1877–87
[44] Lu D, Vishik I, Yi M, Chen Y, Moore R and Shen Z 2012 *Annu. Rev. Condensed Matter Phys.* **3** 129–67
[45] Osterwalder J 2006 Spin-polarized photoemission *Magnetism: A Synchrotron Radiation Approach* (*Lecture Notes in Physics* vol 697) ed E Beaurepaire *et al* (Berlin: Springer) pp 95–120
[46] Mott N F 1986 *A Life in Science* (London: Taylor and Francis)
[47] Hume-Rothery W 1931 *The Metallic State* (Oxford: Oxford University Press)
[48] Mott N F 1987 *Biographical Mem. Fellows R. Soc.* **33** 326–42
[49] Jones H 1934 *Proc. R. Soc.* A **144** 225–34
[50] Jones H 1937 *Proc. Phys. Soc.* **49** 250
[51] Paxton A T, Methfessel M and Pettifor D G 1997 *Proc. R. Soc.* A **453** 1493–514
[52] Mizutani U 2010 *Hume-Rothery Rules for Structurally Complex Alloy Phases* (Boca Raton, FL: CRC Press)
[53] Blandin A 1963 *Alloying Behaviour and Effects in Concentrated Solid Solutions* ed T Massalski (New York: Gordon and Break) pp 50–78
[54] Blandin A 1967 *Phase stability in Metals and Alloys* ed P Rudman *et al* (New York: McGraw-Hill) p 115
[55] Heine V 1969 *The Physics of Metals* vol 1 ed J Ziman (Cambridge: Cambridge University Press) pp 1–61
[56] Stroud D and Ashcroft N W 1971 *J. Phys. F: Met. Phys.* **1** 113
[57] Evans R, Lloyd P and Mujibur R 1979 *J. Phys. F: Met. Phys.* **9** 1939
[58] Lindhard J 1954 *Dan. Mat. Fys. Medd.* **28** 1–57
[59] Heil C, Sormann H, Boeri L, Aichhorn M and von der Linden W 2014 *Phys. Rev.* B **90** 115143
[60] Kohn W 1959 *Phys. Rev. Lett.* **2** 393–4
[61] Woll E J and Kohn W 1962 *Phys. Rev.* **126** 1693–7
[62] Brockhouse B N, Arase T, Caglioti G, Rao K R and Woods A D B 1962 *Phys. Rev.* **128** 1099–111
[63] Gold A V 1958 *Phil. Trans. R. Soc.* A **251** 85–112
[64] Ruderman M A and Kittel C 1954 *Phys. Rev.* **96** 99–102
[65] Kasuya T 1956 *Prog. Theor. Phys.* **16** 45–57
[66] Yosida K 1957 *Phys. Rev.* **106** 893–8
[67] Taylor P L 1963 *Phys. Rev.* **131** 1995–9
[68] Afanas'ev A and Kagan Y 1963 *Sov. Phys.—JETP* **16** 1030
[69] Roth L M, Zeiger H J and Kaplan T A 1966 *Phys. Rev.* **149** 519–25
[70] Weymouth J W and Stedman R 1970 *Phys. Rev.* B **2** 4743–51
[71] Overhauser A W 1962 *Phys. Rev.* **128** 1437–52
[72] Overhauser A W 1963 *J. Appl. Phys.* **34** 1019–24
[73] Lomer W M 1962 *Proc. Phys. Soc.* **80** 489
[74] Fawcett E 1988 *Rev. Mod. Phys.* **60** 209–83
[75] Schwartzman K, Fry J L and Zhao Y Z 1989 *Phys. Rev.* B **40** 454–60
[76] Koehler W C, Moon R M, Trego A L and Mackintosh A R 1966 *Phys. Rev.* **151** 405–13
[77] Kallin C 2012 *Rep. Prog. Phys.* **75** 042501
[78] Mazin I I and Singh D J 1999 *Phys. Rev. Lett.* **82** 4324–7
[79] Iida K *et al* 2011 *Phys. Rev.* B **84** 060402
[80] Friedel J 1958 *Nuovo Cimento* **7** 287–311 (1955–1965)
[81] Winkelmann A, Tusche C, Akin Ünal A, Ellguth M, Henk J and Kirschner J 2012 *New J. Phys.* **14** 043009
[82] Crommie M, Lutz C and Eigler D 1993 *Nature* **363** 524
[83] Weismann A, Wenderoth M, Lounis S, Zahn P, Quaas N, Ulbrich R G, Dederichs P H and Blügel S 2009 *Science* **323** 1190–3
[84] Lounis S, Zahn P, Weismann A, Wenderoth M, Ulbrich R G, Mertig I, Dederichs P H and Blügel S 2011 *Phys. Rev.* B **83** 035427
[85] Johannes M D and Mazin I I 2008 *Phys. Rev.* B **77** 165135
[86] Zhu X, Cao Y, Zhang J, Plummer E W and Guo J 2015 *Proc. Natl Acad. Sci.* **112** 2367–71
[87] Bardeen J, Cooper L N and Schrieffer J R 1957 *Phys. Rev.* **106** 162–4
[88] Anderson P W and Morel P 1961 *Phys. Rev.* **123** 1911–34
[89] Kohn W and Luttinger J M 1965 *Phys. Rev. Lett.* **15** 524–6

[90] Berk N F and Schrieffer J R 1966 *Phys. Rev. Lett.* **17** 433–5
[91] Tsuei C C and Kirtley J R 2000 *Rev. Mod. Phys.* **72** 969–1016
[92] Scalapino D J, Loh E and Hirsch J E 1986 *Phys. Rev.* B **34** 8190–2
[93] Monthoux P, Balatsky A V and Pines D 1991 *Phys. Rev. Lett.* **67** 3448–51
[94] Monthoux P, Pines D and Lonzarich G G 2007 *Nature* **450** 1177–83
[95] Paglione J and Greene R L 2010 *Nat. Phys.* **6** 645–58
[96] Mazin I I, Singh D J, Johannes M D and Du M H 2008 *Phys. Rev. Lett.* **101** 057003
[97] Mazin I I and Schmalian J 2009 *Physica* C **469** 614–27 *Superconductivity in Iron-Pnictides*
[98] Chubukov A and Hirschfeld P J 2015 *Phys. Today* **68** 46
[99] Moss S C 1969 *Phys. Rev. Lett.* **22** 1108–11
[100] Krivoglaz M 1969 *Theory of X-ray and Thermal Neutron Scattering by Real Crystals* (New York: Plenum)
[101] Clapp P C and Moss S C 1966 *Phys. Rev.* **142** 418–27
[102] Clapp P C and Moss S C 1968 *Phys. Rev.* **171** 754–63
[103] Moss S C and Clapp P C 1968 *Phys. Rev.* **171** 764–77
[104] Ohshima K and Watanabe D 1973 *Acta Cryst.* A **29** 520–6
[105] Rodewald M, Rodewald K, De Meulenaere P and Van Tendeloo G 1997 *Phys. Rev.* B **55** 14173–81
[106] Stocks G M, Temmerman W M and Gyorffy B L 1978 *Phys. Rev. Lett.* **41** 339–43
[107] Pindor A, Temmerman W, Gyorffy B and Stocks G 1980 *J. Phys. F: Met. Phys.* **10** 2617
[108] Gyorffy B L and Stocks G M 1983 *Phys. Rev. Lett.* **50** 374–7
[109] Wilkinson I, Hughes R J, Major Z, Dugdale S B, Alam M A, Bruno E, Ginatempo B and Giuliano E S 2001 *Phys. Rev. Lett.* **87** 216401
[110] Takatsu H *et al* 2014 *Phys. Rev.* B **89** 104408
[111] Billington D *et al* 2015 *Sci. Rep.* **5** 12428
[112] Koehler W C 1965 *J. Appl. Phys.* **36** 1078–87
[113] Williams R W, Loucks T L and Mackintosh A R 1966 *Phys. Rev. Lett.* **16** 168–70
[114] Mackintosh A R 1962 *Phys. Rev. Lett.* **9** 90–3
[115] Yosida K and Watabe A 1962 *Prog. Theor. Phys.* **28** 361–70
[116] Loucks T L 1968 *Int. J. Quantum Chem.* **2** 285–90
[117] Loucks T L 1966 *Phys. Rev.* **144** 504–11
[118] Dugdale S B, Fretwell H M, Alam M A, Kontrym-Sznajd G, West R N and Badrzadeh S 1997 *Phys. Rev. Lett.* **79** 941–4
[119] Child H R, Koehler W C, Wollan E O and Cable J W 1965 *Phys. Rev.* **138** A1655–60
[120] Caudron R, Bouchiat H, Monod P, Brown P J, Chung R and Tholence J L 1990 *Phys. Rev.* B **42** 2325–36
[121] Evenson W E and Liu S H 1968 *Phys. Rev. Lett.* **21** 432–4
[122] Evenson W E and Liu S H 1969 *Phys. Rev.* **178** 783–94
[123] Fretwell H M, Dugdale S B, Alam M A, Hedley D C R, Rodriguez-Gonzalez A and Palmer S B 1999 *Phys. Rev. Lett.* **82** 3867–70
[124] Duffy J A, Dugdale S B, McCarthy J E, Alam M A, Cooper M J, Palmer S B and Jarlborg T 2000 *Phys. Rev.* B **61** 14331–4
[125] Döbrich K M, Bihlmayer G, Starke K, Prieto J E, Rossnagel K, Koh H, Rotenberg E, Blügel S and Kaindl G 2007 *Phys. Rev.* B **76** 035123
[126] Döbrich K M, Bostwick A, McChesney J L, Rossnagel K, Rotenberg E and Kaindl G 2010 *Phys. Rev. Lett.* **104** 246401
[127] Döbrich K M, Bostwick A, Rotenberg E and Kaindl G 2010 *Phys. Rev.* B **81** 012401
[128] Hughes I D, Dane M, Ernst A, Hergert W, Luders M, Poulter J, Staunton J B, Svane A, Szotek Z and Temmerman W M 2007 *Nature* **446** 650–3
[129] Majkrzak C F, Cable J W, Kwo J, Hong M, McWhan D B, Yafet Y, Waszczak J V and Vettier C 1986 *Phys. Rev. Lett.* **56** 2700–3
[130] Grünberg P, Schreiber R, Pang Y, Brodsky M B and Sowers H 1986 *Phys. Rev. Lett.* **57** 2442–5
[131] Baibich M N, Broto J M, Fert A, Van Dau F N, Petroff F, Etienne P, Creuzet G, Friederich A and Chazelas J 1988 *Phys. Rev. Lett.* **61** 2472–5
[132] Fert A, Grünberg P, Barthélémy A, Petroff F and Zinn W 1995 *J. Magn. Magn. Mater.* **140–144** 1–8 Part 1
[133] Parkin S S P, More N and Roche K P 1990 *Phys. Rev. Lett.* **64** 2304–7
[134] Bruno P and Chappert C 1991 *Phys. Rev. Lett.* **67** 1602–5
[135] Bruno P and Chappert C 1992 *Phys. Rev.* B **46** 261–70
[136] Hughes R J, Dugdale S B, Major Z, Alam M A, Jarlborg T, Bruno E and Ginatempo B 2004 *Phys. Rev.* B **69** 174406
[137] Lathiotakis N N, Györffy B L, Bruno E, Ginatempo B and Parkin S S P 1999 *Phys. Rev. Lett.* **83** 215–8
[138] Van Hove L 1953 *Phys. Rev.* **89** 1189–93
[139] Lifshitz I 1960 *Sov. Phys.—JETP* **11** 1130
[140] Blanter Y M, Kaganov M I, Pantsulaya A V and Varlamov A A 1994 *Phys. Rep.* **245** 159–257
[141] Bruno E, Ginatempo B, Guiliano E S, Ruban A V and Vekilov Y K 1994 *Phys. Rep.* **249** 353–419
[142] Haen P, Flouquet J, Lapierre F, Lejay P and Remenyi G 1987 *J. Low Temp. Phys.* **67** 391–419
[143] Daou R, Bergemann C and Julian S R 2006 *Phys. Rev. Lett.* **96** 026401
[144] Bercx M and Assaad F F 2012 *Phys. Rev.* B **86** 075108
[145] Aoki D, Huxley A, Ressouche E, Braithwaite D, Flouquet J, Brison J P, Lhotel E and Paulsen C 2001 *Nature* **413** 613–6
[146] Lévy F, Sheikin I, Grenier B and Huxley A D 2005 *Science* **309** 1343–6
[147] Yelland E A, Barraclough J M, Wang W, Kamenev K V and Huxley A D 2011 *Nat. Phys.* **7** 890–4
[148] Aoki D, Knebel G and Flouquet J 2014 *J. Phys. Soc. Japan* **83** 094719
[149] Grigera S A, Perry R S, Schofield A J, Chiao M, Julian S R, Lonzarich G G, Ikeda S I, Maeno Y, Millis A J and Mackenzie A P 2001 *Science* **294** 329–32
[150] Lester C, Ramos S, Perry R S, Croft T P, Bewley R I, Guidi T, Manuel P, Khalyavin D D, Forgan E M and Hayden S M 2015 *Nat. Mater.* **14** 373–8
[151] Ni N, Bud'ko S L, Kreyssig A, Nandi S, Rustan G E, Goldman A I, Gupta S, Corbett J D, Kracher A and Canfield P C 2008 *Phys. Rev.* B **78** 014507
[152] Ronning F, Klimczuk T, Bauer E D, Volz H and Thompson J D 2008 *J. Phys.: Condens. Matter.* **20** 322201
[153] Canfield P C, Bud'ko S L, Ni N, Kreyssig A, Goldman A I, McQueeney R J, Torikachvili M S, Argyriou D N, Luke G and Yu W 2009 *Physica* C **469** 404–12 *Superconductivity in Iron-Pnictides*
[154] Soh J H *et al* 2013 *Phys. Rev. Lett.* **111** 227002
[155] Yildirim T 2009 *Phys. Rev. Lett.* **102** 037003
[156] Gofryk K, Saparov B, Durakiewicz T, Chikina A, Danzenbächer S, Vyalikh D V, Graf M J and Sefat A S 2014 *Phys. Rev. Lett.* **112** 186401
[157] Jani M, Leary M, Subic A and Gibson M 2014 *Mater. Des.* **56** 1078–113
[158] Shapiro S M, Larese J Z, Noda Y, Moss S C and Tanner L E 1986 *Phys. Rev. Lett.* **57** 3199–202
[159] Zhao G L and Harmon B N 1992 *Phys. Rev.* B **45** 2818–24
[160] Dugdale S B, Watts R J, Laverock J, Major Z, Alam M A, Samsel-Czekała M, Kontrym-Sznajd G, Sakurai Y, Itou M and Fort D 2006 *Phys. Rev. Lett.* **96** 046406
[161] Shiotani N, Matsumoto I, Kawata H, Katsuyama J, Mizuno M, Araki H and Shirai Y 2004 *J. Phys. Soc. Japan* **73** 1627–30
[162] Goddard P A, Singleton J, McDonald R D, Harrison N, Lashley J C, Harima H and Suzuki M T 2005 *Phys. Rev. Lett.* **94** 116401
[163] McDonald R D *et al* 2005 *J. Phys.: Condens. Matter.* **17** L69

[164] Webster P J, Ziebeck K R A, Town S L and Peak M S 1984 *Phil. Mag.* B **49** 295–310
[165] Velikokhatnyi O and Naumov I 1999 *Phys. Solid State* **41** 617–23
[166] Lee Y, Rhee J Y and Harmon B N 2002 *Phys. Rev.* B **66** 054424
[167] Zheludev A, Shapiro S M, Wochner P, Schwartz A, Wall M and Tanner L E 1995 *Phys. Rev.* B **51** 11310–4
[168] Haynes T D, Watts R J, Laverock J, Major Z, Alam M A, Taylor J W, Duffy J A and Dugdale S B 2012 *New J. Phys.* **14** 035020
[169] Canfield P C, Gammel P L and Bishop D J 1998 *Phys. Today* **51** 40–6
[170] Cava R J *et al* 1994 *Nature* **367** 252–3
[171] Siegrist T, Zandbergen H W, Cava R J, Krajewski J J and Peck W F 1994 *Nature* **367** 254–6
[172] Zehetmayer M 2013 *Supercond. Sci. Technol.* **26** 043001
[173] Sinha S K, Lynn J W, Grigereit T E, Hossain Z, Gupta L C, Nagarajan R and Godart C 1995 *Phys. Rev.* B **51** 681–4
[174] Zarestky J, Stassis C, Goldman A I, Canfield P C, Dervenagas P, Cho B K and Johnston D C 1995 *Phys. Rev.* B **51** 678–80
[175] Lynn J W, Skanthakumar S, Huang Q, Sinha S K, Hossain Z, Gupta L C, Nagarajan R and Godart C 1997 *Phys. Rev.* B **55** 6584–98
[176] Dervenagas P, Zarestky J, Stassis C, Goldman A I, Canfield P C and Cho B K 1996 *Phys. Rev.* B **53** 8506–8
[177] Detlefs C, Goldman A I, Stassis C, Canfield P C, Cho B K, Hill J P and Gibbs D 1996 *Phys. Rev.* B **53** 6355–61
[178] Dervenagas P, Bullock M, Zarestky J, Canfield P, Cho B K, Harmon B, Goldman A I and Stassis C 1995 *Phys. Rev.* B **52** R9839–42
[179] Rhee J Y, Wang X and Harmon B N 1995 *Phys. Rev.* B **51** 15585–7
[180] Kohara T *et al* 1995 *Phys. Rev.* B **51** 3985–8
[181] Wills A S, Detlefs C and Canfield P C 2003 *Phil. Mag.* **83** 1227–34
[182] Lamago D, Hoesch M, Krisch M, Heid R, Bohnen K P, Böni P and Reznik D 2010 *Phys. Rev.* B **82** 195121
[183] Dugdale S B, Alam M A, Wilkinson I, Hughes R J, Fisher I R, Canfield P C, Jarlborg T and Santi G 1999 *Phys. Rev. Lett.* **83** 4824–7
[184] Dugdale S B, Utfeld C, Wilkinson I, Laverock J, Major Z, Alam M A and Canfield P C 2009 *Supercond. Sci. Technol.* **22** 014002
[185] Starowicz P *et al* 2008 *Phys. Rev.* B **77** 134520
[186] Chang J *et al* 2012 *Nat. Phys.* **8** 871–6
[187] Katayama-Yoshida H, Koyanagi T, Funashima H, Harima H and Yanase A 2003 *Solid State Commun.* **126** 135–9